Drashtikon: Extra Ocular Disease Classification

Shloka Desai (shloka), Zachary Maurer, (zmaurer), Chelsea Sidrane,(csidrane)

December 17, 2016

Abstract

This work outlines the development of a classifier for extra ocular conditions that uses natural, noisy images of faces taken with point-and-shoot cameras. The entire dataset consists of about 7,244 labeled images of patients from Drashti Netralaya Eye Hospital in Gujarat, India. Five diseases were selected for classification: Goonderson Flap, Dermoid Cyst, Strabismus, Ptosis, and Ocular Surface Disease. Histogram of Oriented Gradient feature descriptors were utilized with Support Vector Machines and Logistic Regression. Modern Neural Network architectures were also applied. Bottleneck CNN and Logistic Regression (Balanced) both performed well according to different error measurements. The Bottleneck CNN achieved the highest test accuracy of 77% but Logistic Regression had the highest true positive rate averaged across all classes. Thus, it is possible to develop a classifier from everyday images for a variety of eye diseases. More research is necessary to develop robust predictive capabilities across all diseases.

1 Introduction

This work outlines the development of a classifier for extra ocular conditions that uses natural, noisy images of faces taken with point-and-shoot cameras. Extra ocular conditions are disorders that affect the outside of the eye, as opposed to intra ocular diseases which affect internal components such as the retina. Ophthalmologists are able to diagnose many extra ocular conditions without examining the internals of the eye. Thus, we believe that these external images will provide a sufficiently rich data set for making predictions.

2 Previous Work

The majority of existing research on using machine learning techniques to detect eye diseases in images of a person's eye or face are taken with specialized camera equipment or utilize specialized diagnostic data.[8] These efforts have generally utilized models like Support Vector Machines (SVM) and neural networks (NNs) to make predictions.[8] Research has also been done on classifying retinal scans/images for particular diseases, such as diabetic retinopathy, which can lead to blindness.[6,10] There are ongoing efforts between Google DeepMind and the NHS to evaluate automated techniques for interpreting more specialized eye scans.[7] There have also been efforts to build a web-based diagnostic systems for diabetic retinopathy relying on human experts in order to identify early onset of the disease.[11, 14] However, there seem to be comparatively few research studies on diagnosing extra ocular conditions, especially for photos that are not taken with specialized equipment. Most previous work also involves detecting the presence or absence of a single eye condition, as opposed to classifying multiple different eye disorders. Thus, we believe that our work: attempting to build a multi-class extra ocular eye disease classifier by applying modern methods to a heterogeneous image dataset taken with point-and-shoot cameras, will be a welcome extension on existing research.

2.1 Dataset

The entire dataset consists of about 7,244 labeled images of patients from Drashti Netralaya Eye Hospital in Gujarat, India. Five diseases were selected for classification: Goonderson Flap, Dermoid Cyst, Strabismus, Ptosis, and Ocular Surface Disease.

The images were pre-processed before they were passed to the classifier. Facial landmark features in each image were located, and then the images were cropped to 150x300, and transformed so that the eyes were centered and level in the frame. This processing was done using OpenFace[3] and Dlib[2]. The last step was to normalize the image histogram in order to increase the contrast of the image using the Pillow image processing library.[1] After pre-processing, the dataset consisted of 5,058 labeled images. Eighty percent of the images were used for training and twenty percent were used for testing. A table of image distributions are below.

Table 1: Class Totals

Dermoid Cyst	**Goonderson Flap**	**OSD**	**Ptosis**	**Strabismus**
188	87	590	1571	2622

3 Features

Histogram of Oriented Gradients, or HOG features, were chosen for this project because they have proven very successful for object recognition. In addition, HOG features are resistant to changes in exposure, which was an asset since the exposure of different images in

the dataset varied widely. To avoid our models learning from irrelevant artifacts in the original 150x300 image, we also generated another set of features called 'cropped HOG'. To generate these we extracted HOG features from tightly cropped images of each eye (cropped to 96x96) and concatenated the feature vectors together. The ordering of feature extraction and then concatenation was intended to avoid the introduction of new image artifacts from extracting HOG features from the concatenation of two discontinous regions of a photograph. For reasons that will be elaborated on later, Principle Components Analysis (PCA) was also used to reduce the dimensionality of the feature space. Lastly, we confirmed that HOG features performed better than the mean brightness of the image, which was chosen as a baseline comparison and yielded classification only slightly better than chance.

Figure 1: Sample preprocessing of an image to extract HOG and cropped HOG features

4 Methods

4.1 Conventional Models

Three different models – SVM with a Linear kernel, SVM with an RBF kernel and Logistic Regression – were used because they reflect previous work on this subject, and these classifiers are easy to use with the continuous-valued HOG features. The cost function, loss, and kernel are given as follows for the SVM with a Linear Kernel:
$J_\lambda(\alpha) = \frac{1}{m}\sum_{i=1}^{m} L(K^{(i)T}\alpha, y^{(i)}) + \frac{\lambda}{2}\alpha^T K\alpha$, $L(z,y) = \max\{0, 1-yz\}$, $K(x,z) = x^T z$.
For the SVM with a Radial Basis function (RBF), the kernel is given by $K(x,z) = exp(\frac{-1}{2\tau^2}||x-z||_2^2)$.
For Logistic Regression the cost function is given by $\frac{1}{2}\sum_{i=1}^{m}\left(\frac{1}{1+e^{-\theta^T x}} - y^{(i)}\right)^2$.

For each of these, a balanced version of the model was also used, which automatically adjusts weights inversely proportional to class frequencies in the input data. These models were implemented using Python's Scikit Learn library.[4]

4.2 Neural Network

In addition, different architectures of a Convolutional Neural Network were developed using Keras and Tensorflow, based on the information found on the Keras blog.[12] The different architectures we used were:

- **Simple CNN**: This is a very basic neural network with three layers of 32, 32, and 64 units respectively. Each of these layers has ReLu (Rectified Linear Unit) and maxpooling layers (to reduce dimensionally). Two dense layers were added on top and a final unit using sigmoid activation was used for making predictions. The loss we used was binary crossentropy.
- **Bottleneck CNN**: This CNN used the bottleneck features generated by running the images from the dataset once through VGG16 (a 16-layer neural network used by the VGG team in the ILSVRC-2014 competition), instantiated only for the convolutional layers. These features were then used to train a fully connected CNN. The net has a fully connected layer followed by a dropout layer (for regularization) and a final prediction unit with sigmoid-softmax activation for multi-class predictions. This CNN also uses binary crossentropy for loss (categorical crossentropy for multiclass) and accuracy as the training metric. We used RMSprop as the optimizer for binary classification but this resulted in a sudden drop in accuracy during training for the multiclass case. We tried several other optimizers (stochastic gradient descent, Adam), and Adam turned out to be the most performant.
- **VGG16 (Topmost Layers)**: In this model, we fine tuned the last convolutional block of VGG16 along with the fully connected CNN and froze all the other layers for VGG16 while training. We used Stochastic Gradient Descent as the optimizer and accuracy as the training metric.

Before training, we also performed data augmentation on the images using Keras's ImageDataGenerator, which generates similar images by rotating, zooming in randomly, translating horizontally or vertically, shearing and randomly horizontally flipping the images.

5 Results

Metrics The F1 score, which is the harmonic mean of precision and recall, was chosen as a performance measure because it reflects the relevance of a given disease classification to an image. While many diagnostic tools use sensitivity and specificity, because we do not consider a "no disease" classification, individual sensitivity and specificity values have less significance. However, the F1 score is biased measure and is affected by the distribution of samples in each category. For that reason, during cross validation and parameter tuning, we used an additional metric, the Area Under Curve of the Receiver Operating Characteristic curve (AUC-ROC) to encourage the selection of "well-rounded" classifiers.

5.1 Initial Exploration: Binary Classification

Linear Classifiers The performance of the selected models was first assessed using a binary classification task to give an estimate of the feasibility of this project, and to predict the situations where a more complicated multi-class model would have difficulty making predictions. For these binary tests, the three disease datasets with the largest number of cropped images were used: Strabismus (str), Ptosis (ptosis), and Ocular Surface Disease (OSD). Initial results using these data demonstrated that SVM models with a Radial Basis Function (RBF) kernel performed the worst. It was suspected that this poor performance was due to a lack of tuned hyperparameters and possibly the high dimensionality of the feature space. The initial results from binary classification are show in the Table 2.

Table 2: Binary Classification Data Subset

Disease Pair	Model	Feature	Single Disease Test Set	Error
str_ptosis	logisticRegressionBalanced	hog	str	0.095602294
str_ptosis	logisticRegressionBalanced	hog	ptosis	0.134185304
str_ptosis	rbfSVMBalanced	hog	str	1
str_ptosis	rbfSVMBalanced	hog	ptosis	0

To examine these results, learning curves were created for the top performing models. A subset of these graphs is shown below. These curves plot the test and train error for models trained on increasing training set sizes which were additively generated and separate from the test set. From these graphs, we hypothesized that our classifiers had high variance because training error was very low and test error much higher.

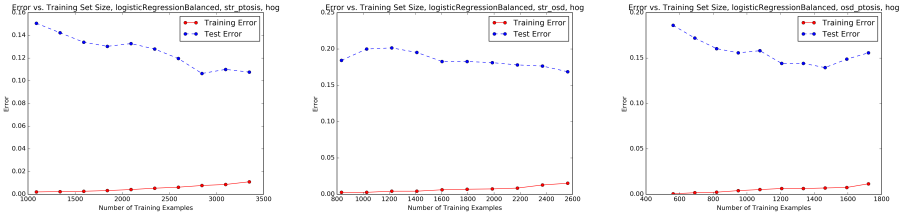

Figure 1: Learning Curves

Neural Network Classification We ran all three neural nets for classifying Ptosis vs. Strabismus. All three neural nets overfit the training data. During training we saw that Simple CNN achieved around 84% after 500 epochs (the exact accuracy was 84.1% for training, and 79% test accuracy). The top layer CNN using VGG16 had around 92% accuracy during training after 100 epochs. The bottleneck CNN performed the best, with a train accuracy of 98% and a test accuracy of 88%. We ran the Bottleneck CNN for the multiclass case because it ran in under 5 minutes, as opposed to the top layer CNN which took around 18 hours to run 200 epochs.

5.2 Model Refinement: Multi-Class Classification

Following the initial exploratory model development, all selected models were tested for the multiclass case with five diseases: Strabismus, OSD, Ptosis, Goonderson Flap, Dermoid Cyst. The best performing classifier with standard HOG features was Logistic Regression (Balanced). See Table 3.

Linear Classifiers Drawing on the conclusions from the learning curves derived from the binary classifiers, we sought to reduce the variance of our models by (1) introducing 'cropped-hog' features (which reduces the size of the original image and consequently the number of HOG descriptor values) and (2) applying Principal Components Analysis to our features to reduce their dimensionality. These results are presented in the bottom rows of Table 3.

Table 3: Initial Results

Model	Feature	F1 Score (micro average)
Logistic Regression (Balanced) (C=1.0)	HoG	**0.774**
Logistic Regression (C=1.0)	HoG	0.766
Linear SVM (Balanced) (C=1.0)	HoG	0.768
Linear SVM (C=1.0)	HoG	0.767
RBF SVM (C=1.0, gamma=0.00002)	HoG	0.52
RBF SVM (Balanced) (C=1.0, gamma=0.00002)	HoG	0.016
Logistic Regression (Balanced) (C=1.0)	Cropped HoG	**0.775**
Logistic Regression (Balanced)(C=1.0)	HoG, PCA (n=4037)	**0.775**
Logistic Regression (Balanced) (C=1.0)	Cropped HoG, PCA (n=4037)	0.744

Logistic Regression (Balanced) using cropped HOG features, and Logistic Regression (Balanced) using HOG features and a PCA reduction to 4,037 principle components compared very similarly to Logistic Regression (Balanced) with standard HOG features.

Once the performance of PCA-transformed features was established as reasonable, estimates for the ideal number of principle components were obtained by plotting the fraction of explained variance as a function of the number principal components. These plots are shown below. The key take-away is that there is minimal variance explained beyond 1000-2000 principal components.

Cross Validation and Grid Search To improve upon these results, 5-fold cross validation was performed using exhaustive grid search to tune the hyperparamaters of all multi-class models listed above. AUC-ROC was used as the cross validation scoring metric. This was designed to correct for the imbalance of class examples, as explained in the Metrics section. The best models resulting from evaluating 40-150 candidate tunings for each classifier is listed in Table 4.

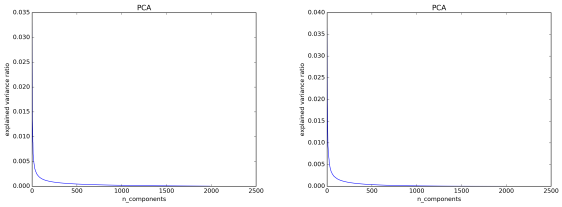

Figure 2: Fraction of explained variance curves for different feature sets. Five disease classes: strabismus, osd, ptosis, goonderson flap, dermoid cyst

Most notably, there was significant improvement in the performance of the RBF-SVM. However, despite these improvements, Logistic Regression performed more poorly with 1000 or 2000 principal components than with a greater number of features, as previously observed. This is likely due to the loss in predictive signal caused by reducing the number of principal components. As a final tuning step, the best hyperparameters for each model that were derived from cross validation were then applied to models which trained on the full set of uncompressed cropped HOG features.

Table 4: Cross-Validation Results

Best CV Model	**Best CV Feature**	**F1 Score**	**CV AUC Score**
Logistic Regression (C=1.0)	Cropped HoG, PCA (n=1000)	0.7355864811	0.8701992429
RBF SVM (C=1000, gamma=1.0)	Cropped HoG, PCA (n=1000)	0.781312127	0.872994208
Linear SVM (C=0.01)	Cropped HoG, PCA (n=1000)	0.709741551	0.855697867

Final Results The best classifiers chosen using model selection are compared in Table 5. The best performing multiclass classifier was the BottleNeck CNN when comparing using the F1 score, the area under ROC curve computed during validation, and the accuracy.

Table 5: Final Results

Model	**Feature**	**F1 Score**	**CV AUC Score**	**Test Accuracy**
BottleNeck CNN (Adam optimizer, image augmentation)	150 x 300 images	0.773359841	0.8985269319	77.34%
RBF SVM (C=1000, gamma=1.0)	Cropped HoG	0.7574552684	0.8912797333	75.746%
RBF SVM Balanced (C=1000, gamma=1.0)	Cropped HoG	0.7574552684	0.8912123548	75.746%
Logistic RegressionBalanced (C=1.0)	Cropped HoG	0.7465208748	0.8864347028	74.652%
Logistic Regression (C=1.0)	Cropped HoG	0.7365805169	0.882775602	73.658%

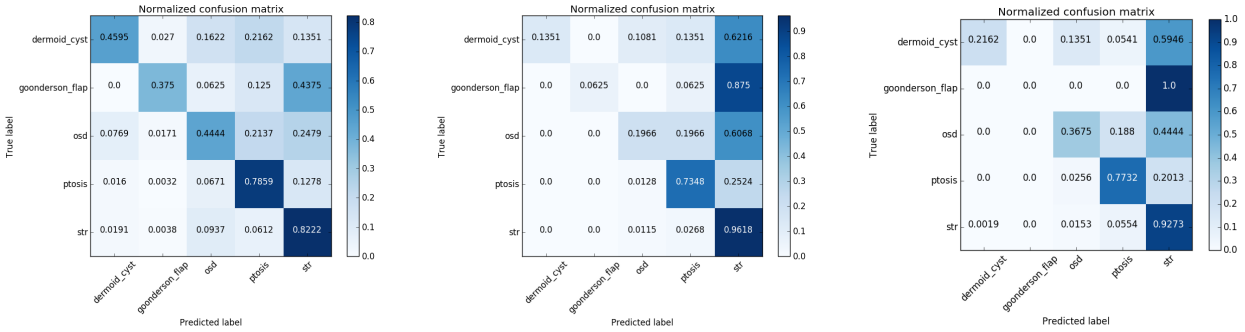

(a) Logistic Regression Balanced (b) RBF-SVM Balanced (c) Bottleneck CNN

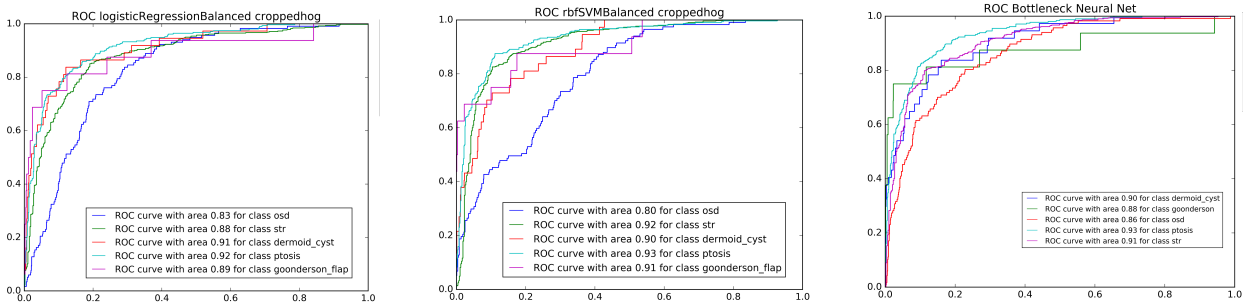

(d) Logistic Regression Balanced (e) RBF-SVM Balanced qquad (f) Bottleneck CNN

Figure 3: Confusion matrices and ROC curves for the best three final models

6 Analysis & Discussion

In this paper, we have demonstrated an iterative tuning effort to produce classifiers that best classify extra occular diseases from conventional images of people's faces.

- **Suspected high variance**
  It was suspected that initial poor performance of the RBF-SVM was due to a lack of tuned hyperparameters(radius for the RBF was too large) and the large number (45,000) of features. In addition, the learning curves suggested that logistic regression may had high variance. Hyperparameter tuning and use of PCA-reduced features (Table 4) was so successful that the RBF-SVM ranked above Logistic Regression and the Linear SVM among the candidates tried in the parameter search. As a result, cross-validation for the RBF-SVM using the first 2000 principle components of the data was tried, but 1000 principle components yielded a higher AUC score. In contrast, the performance of logistic regression and the linear svm, according to the F1 score, was significantly reduced from models using full HOG features. These results may be interpreted to mean that the radial basis function initially had too large of a radius and wasn't able to construct a complicated enough decision surface. As the F1 score for the RBF-SVM and the AUC score got respectively worse and better when removing PCA, we are not able to conclude whether there was high variance in this model. It is possible to conclude that there was likely not high variance in logistic regression and the linear SVMs as removing PCA increased the F1 scores and AUC scores for these models.
- **Redistribution of Error**
  Through our tuning efforts, absolute gains were made for the CNN and the RBF-SVM models. However, for most other models, tuning exchanged the distribution of errors across different classes, as opposed to producing a classifier with truly better predictive capability for all diseases. Although not picture here, tuning the Logistic Regression model through cross-validation in attempt to pick the optimal number of PCA-reduced components produced a classifier that misclassifies almost all Dermoid Cyst and Goonderson Flap examples, while the model without PCA tuning (Fig. 3) has accuracy $\tilde{4}$0-50% on those classes. We believe this to attributable to overfitting during cross validation or a loss of signal due to PCA transformation.
- **Neural Net Performance**
  By the metrics used here, the bottleneck CNN performed the best out of all classifiers. However, this minor gain comes as the price of misidentifying almost all Dermoid Cyst and Goonderson Flap examples, as demonstrated in the confusion matrix in Fig. 3. However from examining the ROC curve of the neural net (Fig.3) it is clear that the neural net does better than the other classifiers at identifying OSD. If a classifier is desired that accurately classifies Goonderson flap, if, for example, a certain population is deemed to be at risk if they were to develop this disorder, then logistic regression would be a better classifier than the neural net, and vice-versa if a classifier that prioritizes OSD is desired.
- **Consistency in Errors**
  Strabismus and Ptosis were the most accurately identified diseases across all classifiers. Despite have many training examples, OSD was misclassified the third most often. This is likely due to OSD being the smallest visible defect of all the diseases examined in this project. Specifically, OSD is a very small abberation on the cornea, often appearing like a small watery patch. OSD and Ptosis diseases have much larger, recognizable symptoms. Dermoid Cyst and Goonderson Flap also manifest with pronounced symptoms, but, as noted, the number of examples for those classes were much smaller.
- **Neural Network Overfitting** In general we saw that all the neural networks overfit the data. To fix this in future iterations we can use L1/L2 regularization, dropout and weight decay. The multiclass classifier does really well for the classes which have a lot of training images, the only way to improve the accuracy for the other classes would be to add images. We used data augmentation but it does not help in this case because the training set size for some of the classes is really small.

7 Conclusion

Linear classifiers such as logistic Regression (Balanced) perform similarly to modern neural network architechtures such as a bottleneck CNN in classifying Strabismus, Ocular Surface Disease, Ptosis, Goonderson Flap, and Dermoid Cyst from natural, noisy images of faces taken with non-specialized equipment. Use of these two models in combination with HOG features extracted from the region around the eyes yields test accuracy of 75-77%. Better diagnostic accuracy would be required for deployment in a real system but this proof-of-concept system demonstrates that automatic classification of this type is possible.

8 Future Work

In the future we hope to be able to improve our results by pursuing several extensions to our work. We could refine preprocessing, specifically the step where we identify the region corresponding to the eye, to utilize more of the original dataset. To improve the accuracy of the existing neural network, we could try obtaining more images for some of the smaller datasets (for example Goonderson flap) and try running VGG16 and the simple CNN for longer iterations. We could also try and reduce the overfitting by using several methods such as dropout, more aggresive data augmentation and using of L1 and L2 regularization.
Apart from making changes to the existing infrastructure, we could also obtain more data to classify whether a patient has an eye disease or is healthy (no disease), and we could classify some of the other more common eye diseases that don't necessarily need surgery (like conjunctivitis, stye etc.). This would make our classifier more useful.

References

[1] **Python Image Library**. https://python-pillow.org

[2] **Dlib Library**. http://dlib.net

[3] **OpenFace Facial Recognition**. https://cmusatyalab.github.io/openface

[4] **Scikit Framework**. http://scikit-learn.org/stable

[5] **Comparing Machine Learning Classifiers for Diagnosing Glaucoma from Standard Automated Perimetry**.
http://iovs.arvojournals.org/article.aspx?articleid=2123399

[6] **Machine learning and pattern classification in identification of indigenous retinal pathology**.
http://ieeexplore.ieee.org/document/6091471/?arnumber=6091471

[7] **Moorfields announces research partnership**. http://www.moorfields.nhs.uk/news/moorfields-announces-research-partnership

[8] **Computional methodology for automatic detection of strabismus in digital images through Hirschberg test**.
http://www.sciencedirect.com/science/article/pii/S0010482511002149

[9] **Applied Artificial Intelligence Techniques for Identifying the Lazy Eye Vision Disorder**.
https://www.degruyter.com/view/j/jisys.2011.20.issue-2/jisys.2011.007/jisys.2011.007.xml

[10] **Evaluation of a system for automatic detection of diabetic retinopathy from color fundus photographs in a large population of patients with diabetes**. https://www.ncbi.nlm.nih.gov/pubmed/18024852

[11] **Web-Based Screening for Diabetic Retinopathy in a Primary Care Population: The EyeCheck Project.**
http://connection.ebscohost.com/c/articles/21960239/web-based-screening-diabetic-retinopathy-primary-care-population-eyecheck-project

[12] **Building powerful image classification models using very little data.**
https://blog.keras.io/building-powerful-image-classification-models-using-very-little-data.html

[13] **Receiver Operating Characteristic.** https://en.wikipedia.org/wiki/Receiver_operating_characteristic

[14] **Telemedicine in diabetic retinopathy: Access to rural India.** https://www.ncbi.nlm.nih.gov/pubmed/26953029